THE ASTROPHYSICAL JOURNAL, 471:L41–L44, 1996 November 1

THE COOLING WHITE DWARF IN VW HYDRI AFTER NORMAL OUTBURST AND SUPEROUTBURST: *HST* EVIDENCE OF A SUSTAINED ACCRETION BELT[1]

EDWARD M. SION,[2] FU-HUA CHENG,[2,3] MIN HUANG,[2] IVAN HUBENY,[4] AND PAULA SZKODY[5]
Received 1996 April 22; accepted 1996 August 19

ABSTRACT

Hubble Faint Object Spectrograph (FOS) observations of VW Hyi one day after the end of a normal dwarf nova outburst reveal a heated white dwarf with deep, broad Lyα, narrow metallic absorption features, and evidence of a hotter Keplerian-broadened component manifested in quiescence as a broad continuum hump. Our best reduced χ^2 fit to the data reveals (1) a DAZQ white dwarf with $T_{\rm eff} = 22{,}500 \pm 500$ K, log $g = 8$, and photospheric abundances C = 0.5 solar, N = 5.0 solar, O = 2.0 solar, Si = 0.2 solar, Fe = 0.5 solar, with all other metals being 0.3 solar, and (2) a rapidly spinning accretion belt with $V_{\rm rot} = 3350$ km s^{-1}, $T_{\rm belt} = 26{,}000 \pm 1000$ K, log $g = 6.0$, and a fractional belt area of approximately 11%. Our earlier FOS spectrum obtained 10 days after superoutburst reveals a cooler DAZQ white dwarf (20,500 ± 1000 K), relatively lower metal abundances, and a smaller fractional area (3%) for the accretion belt. Thus, 1 day after a normal outburst, the white dwarf is ≈2000 K hotter, the accretion belt fractional area is a factor of 3 greater, the accretion belt temperature appears to be cooler than at 10 days post-superoutburst, and the accreted atmosphere has relatively higher metal abundances. Finally, the accretion belt maintained during quiescence may provide a natural explanation for the 14 s soft X-ray oscillations, requires a deeper source of heating (compression and shear mixing), and implies a lower limit to the viscous spin-down timescale of 10 days.

Subject headings: novae, cataclysmic variables — stars: individual (VW Hydri) — white dwarfs

1. INTRODUCTION

Accretion belts should be a natural consequence of tangential accretion onto a white dwarf (Kippenhahn & Thomas 1978), but have never been identified spectroscopically. Among dwarf novae with exposed white dwarfs, the SU UMa–type dwarf nova VW Hyi is nearly ideal for a search because it undergoes both normal outbursts (NOBs) and superoutbursts (SOBs), as well as clearly revealing its white dwarf during quiescence (Mateo & Szkody 1984; Sion et al. 1995a, 1995b) as the dominant far-UV flux source. *HST* spectroscopic determinations of the white dwarf $T_{\rm eff}$, log g, photospheric chemical abundances, and axial rotation rate have been reported (Sion et al. 1995a, 1995b). The signature and contribution of UV-emitting gas in Keplerian motion near or on the white dwarf during quiescence have been characterized (Huang et al. 1996b). In this Letter we report an analysis of a second FOS spectrum obtained only 1 day after a normal outburst (hereafter post-NOB), comparatively analyzed with an earlier post-superoutburst (hereafter post-SOB) FOS spectrum.

[1] Based on observations with the NASA/ESA *Hubble Space Telescope*, obtained at the Space Telescope Science Institute, which is operated by the Association of Universities for Research in Astronomy, Inc., under NASA contract NAS5-26555.

[2] Department of Astronomy and Astrophysics, Villanova University, Villanova, PA 19085; emsion@ucis.vill.edu.

[3] Center for Astrophysics, University of Science and Technology in China, Hefei, Anhui 230026, People's Republic of China.

[4] Laboratory for Astronomy and Solar Physics, Code 681, NASA/GSFC, Greenbelt, MD 20771; hubeny@tlusty.gsfc.nasa.gov.

[5] Department of Astronomy, University of Washington, Seattle, WA 98195; szkody@astro.washington.edu.

2. *HST* FOS OBSERVATIONS

The *Hubble* FOS observation was carried out on 1995 January 28 (19:33:01 UT), approximately 1 day after the return to optical quiescence following a normal outburst which began on day 24 (1995 January 24). The observation was obtained with the following instrumental setup: the G130H grating with blue Digicon and the 1″ circular aperture, giving resolving power of 1200 and a wavelength coverage of 1150–1600 Å. The target acquisition was carried out with no apparent difficulties. The total exposure time was 720 s with the start time at MJD = 49,745.81177279 and the end time at MJD = 49,745.82030201. Using the photometric ephemeris of van Amerongen et al. (1987) (where phase 0.0 corresponds to approximately phase 0.73 in an ephemeris with zero phase defined as inferior conjunction of the secondary), the corresponding orbital phases at the start and end of the exposure are 0.07 and 0.19, respectively.

The spectrum (shown in Fig. 1) has a signal-to-noise ratio of 7:1 and was reduced through the standard STScI pipeline processing. The flux level is consistent with the flux level of our earlier FOS spectra (Sion et al. 1995a) and low-resolution *IUE* spectra of VW Hyi in optical quiescence (cf. Mateo & Szkody 1984). We see in Figure 1 the very broad Lyα absorption profile and a rich metallic absorption spectrum with the strongest metal features labeled similar to our earlier FOS spectrum obtained 10 days post-SOB (see Sion et al. 1995a). There is a weak, narrow emission feature due to the Lyα geocoronal feature. Its narrow width makes it unlikely that VW Hyi itself is contributing to the emission. There is also a moderately strong, broad C IV emission line associated with the Keplerian broadening of an accretion disk. The strength and breadth of the neutral and singly ionized metallic absorption features, in view of the low interstellar column in the line of sight to VW Hyi, rule out an interstellar origin.

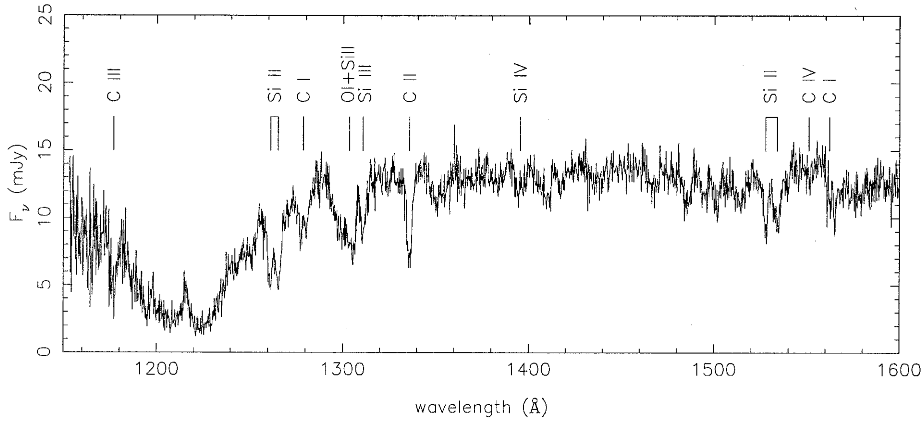

FIG. 1.—Second FOS spectrum (1 day post-NOB), displayed with the strongest metal absorption features marked.

3. SYNTHETIC SPECTRAL FITTING

There are several important differences between this new FOS spectrum and the post-SOB spectrum analyzed in Sion et al. (1995a) and Huang et al. (1996b). In the new spectrum the continuum curvature between 1400 and 1550 Å is flatter and less pronounced, while the overall flux level is a factor of 1.3 higher and the Lyα absorption feature is measurably narrower. The latter two differences almost certainly indicate a higher overall white dwarf surface temperature (1 day post-NOB), while the flatter continuum is consistent with a hotter white dwarf photosphere and/or a reduced contribution from gas with Keplerian broadening. From *HST* spectroscopy of VW Hyi in superoutburst (Huang et al. 1996a) and *IUE* spectra taken in outburst (e.g., Verbunt et al. 1987), it is clearly evident that pronounced continuum curvature between 1380 and 1550 Å is a spectroscopic hallmark of a belt of UV-emitting gas in Keplerian motion near the white dwarf surface. This curvature is still present in spectra at quiescence, but is considerably less pronounced. Thus, any successful composite model in quiescence must consist of a far-UV flux–dominant white dwarf (replicating the broad Lyα wings and core, with the high gravity and moderately slow rotation preserving the narrow photospheric metals), while simultaneously providing the curved continuum signature of a Keplerian broadening component.

The model atmosphere (TLUSTY; Hubeny 1988), model disk (DISKSYN; Hubeny 1995), and spectrum synthesis (SYNSPEC; Hubeny, Lanz, & Jeffrey 1994) codes and details of our χ^2 minimization fitting procedures can be found in Sion et al. (1995a, 1995b) and Huang et al. (1996a, 1996b). For a pair of white dwarf and belt temperatures, we can find a best-fit χ^2 value by adjusting the belt-emitting area. We calculate a grid of χ^2 values for different pairs of white dwarf and belt temperatures, and determine the white dwarf and belt temperatures according to the least χ^2 value.

Our best single-temperature white dwarf model fits to both FOS spectra are summarized in Tables 1 (chemical abundances) and 2 (physical and fitting parameters). Following up our two-temperature models in Huang et al. (1996a, 1996b), to account for the contribution of Keplerian-broadened gas near or on the white dwarf, we attempted white dwarf plus accretion belt fits. We define an accretion belt to mean a rapidly spinning, narrow belt on the white dwarf surface itself, centered at the white dwarf equator. A given belt is constructed by taking appropriate values of log g and $T_{\rm eff}$ for a stellar atmosphere, rotationally broadening the synthetic spectrum to high velocity, and multiplying the fluxes by the fractional area of the belt relative to the white dwarf surface area. We found an improvement in the χ^2 fits when including such a belt in combination with the white dwarf synthetic fluxes. The parameters of our best reduced χ^2 fits to both FOS spectra using white dwarf plus accretion belt fits are given in Table 3. The resulting best fits for the white dwarf alone and for the white dwarf plus accretion belt for the second FOS spectrum obtained 1 day post-NOB are shown in the top and bottom panels, respectively, of Figure 2. Note that the best-fit parameters and chemical abundances of the first FOS spectrum 10 days post-SOB differ slightly from those of Sion et al. (1995a) and Huang et al. (1996b), due to our inclusion of the H_2 quasi-molecular satellite absorption features and a rotational broadening of 300 km s^{-1} in the χ^2 fitting. The best-fitting white dwarf plus accretion belt combination to the first FOS spectrum (10 days post-SOB) is displayed in Figure 3. The accretion belt temperatures span a range from $26{,}000 \pm 1000$ K to $31{,}000 \pm 3000$ K. Hotter belts (e.g., $T_{\rm belt} > 50{,}000$ K) of smaller area are ruled out because Si IV

TABLE 1

WHITE DWARF PHOTOSPHERIC ABUNDANCES (WITH RESPECT TO SOLAR BY NUMBER)

Metal	FOS 1 (10 days post-SOB)	FOS 2 (1 day post-NOB)
C	0.2	0.5
N	3.0	5.0
O	0.5	2.0
Fe	2.0	0.5
Si	0.15	0.2
Other metals	0.15	0.3

TABLE 2

SINGLE WHITE DWARF MODEL FITS

Parameter	FOS 1 (10 days post-SOB)	FOS 2 (1 day post-NOB)
log g	8.0	8.0
$V_{\rm rot}$ (km s^{-1})	300	300
Lyα satellite	Yes	Yes
$T_{\rm wd}$/1000 (K)	22	23.5
Scale factor	2.88×10^{-2}	3.378×10^{-2}
Distance (pc)	72	67
Reduced χ^2	1.58	1.89

TABLE 3

WHITE DWARF PLUS ACCRETION BELT FITS

Parameter	FOS 1 (10 days post-SOB) WD	FOS 1 (10 days post-SOB) Belt	FOS 2 (1 day post-NOB) WD	FOS 2 (1 day post-NOB) Belt
log g	8.0	6.0	8.0	6.0
V_{rot} (km s^{-1})	300	3350	300	3350
Lyα satellite	Yes	Yes	Yes	Yes
T/1000 (K)	20.5 ± 1	31.0 ± 3	22.5 ± 0.5	26.0 ± 1
Scale factor (1×10^{-2})	3.402	0.114	3.453	0.423
Emitting area (%)	96.8	3.20	89.1	10.9
Flux contribution (%)	87.5	12.5	84.0	16.0
Distance (pc)	65		62	
Reduced χ^2	1.56		1.67	

becomes too shallow and the absorption wings vanish, while species like N V become detectable but are not present in the data. Earlier HST analyses of VW Hydri (Huang et al. 1996a, b) and an IUE archival study of VW Hydri by Gansicke and Beuermann (1996) found that two-component models involving a hot equatorial belt can be consistent with the white dwarf spectrum during quiescence. This lends support to the detailed accretion belt analysis we present here.

In both FOS spectra, the best-fitting white dwarf plus accretion belt models corresponded to overabundances of Si (15 solar) and C (20 solar) in the accretion belt. Unless radiative levitation occurs in the belt region or the secondary star has peculiar abundances, we regard these overabundances of C and Si as very preliminary. At this time we have no definitive explanation or interpretation of the enhanced C and Si belt abundances. With more sophisticated spectrum synthesis codes now in development, it is possible these overabundances will not be required in our future detailed fits.

4. DISCUSSION AND CONCLUSIONS

Our synthetic spectral fitting results for the physical state and surface chemistry of the white dwarf and belt 1 day post-NOB have provided a crucial comparison with the characteristics of the white dwarf and belt 10 days post-SOB, analyzed earlier by Sion et al. (1995a) and Huang et al. (1996b). Within the limitations imposed by the signal-to-noise ratio and restricted spectral coverage, our results reveal the following: (1) The white dwarf is hotter by ≈2000 K 1 day post-NOB than the corresponding temperature 10 days post-SOB. (2) The chemical abundances of the white dwarf atmosphere 1 day post-NOB (except for Fe) appear elevated relative to the same elements in the white dwarf atmosphere 10 days post-SOB, i.e., the white dwarf was more metal-enriched 1 day post-NOB than 10 days post-SOB. It is not implausible that only 1 day post-NOB the spectroscopic signature of the injection of freshly accreted matter is stronger than it is 10 days post-SOB because the accreted matter has not had as much time to dilute its chemical abundance through lateral spreading and downward diffusion. (3) The fractional area of the accretion belt we derive at 1 day post-NOB is larger than the fractional area 10 days post-SOB, possibly because of the more recent occurrence of the outburst accretion pulse. (4) The accretion belt temperature 1 day post-NOB is cooler (by 5000 K) than the accretion belt at 10 days post-SOB.

Since the white dwarf in VW Hyi sustains a rapidly spinning accretion belt during quiescence, maintaining its temperature and spin due to repeated accretion episodes every 2–3 weeks, a number of implications follow from the existence of the maintained accretion belt: (1) the presence of a belt up to 10 days post-SOB implies a lower limit to the viscous spin-down timescale of 10 days, and (2) deeper heating is required than the depth of heating associated with a downward-directed

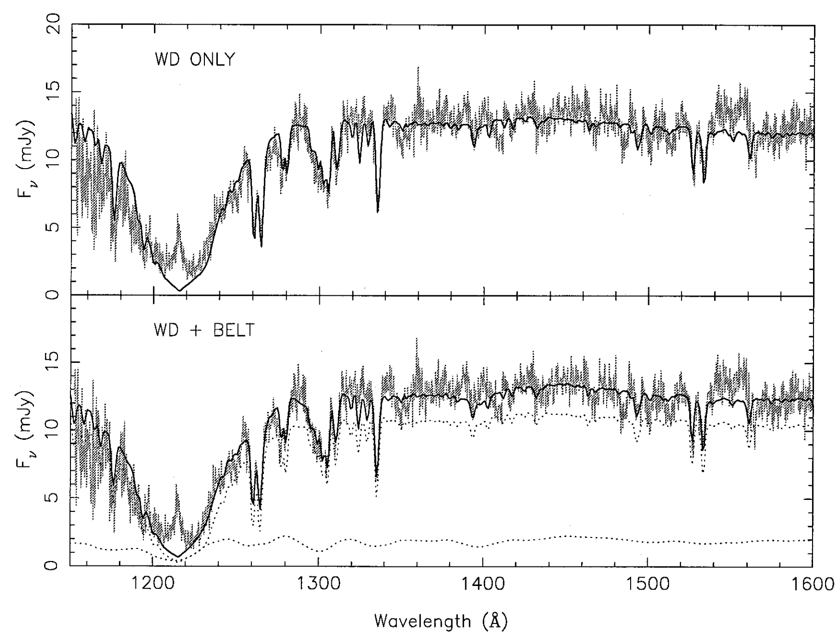

FIG. 2.—*Top*: Best-fit synthetic spectrum of a white dwarf alone, to the new FOS spectrum 1 day post-NOB. (T_{eff} = 23,500 K, log g = 8, $V \sin i$ = 300 km s^{-1}; see text for details.) *Bottom*: Best-fit two-temperature component model (white dwarf plus accretion belt) to the new FOS spectrum. The white dwarf has T_{eff} = 22,500 K, log g = 8.0, and $V \sin i$ = 300 km s^{-1} and contributes 89% of the flux, plus an accretion belt with V = 3350 km s^{-1}, log g = 6; emitting area and flux contribution, 11% and 16%, respectively. The lower dotted line is the contribution of the accretion belt alone, the upper dotted line represents the flux of the white dwarf, and the solid line is the flux combining the white dwarf plus the belt (see text for details).

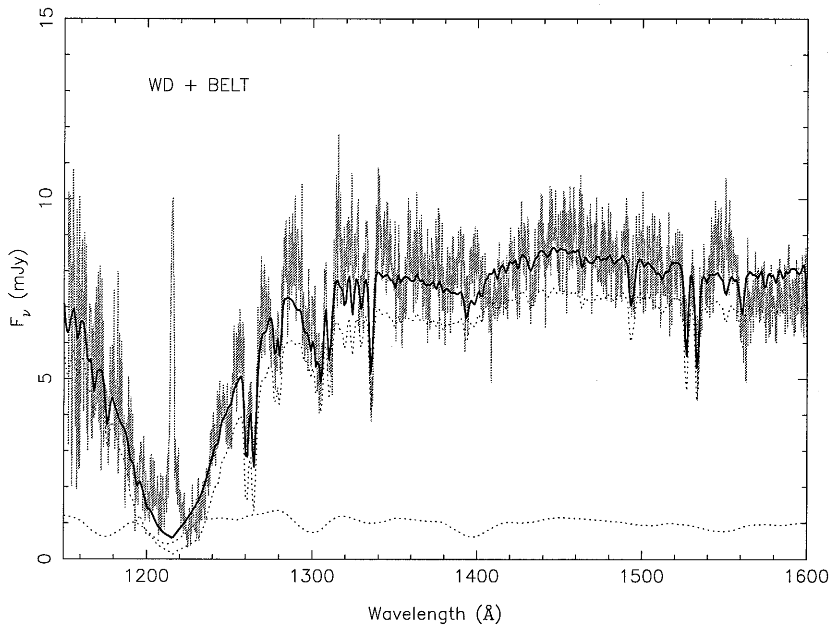

FIG. 3.—FOS spectrum of VW Hyi obtained 10 days post-SOB. The best-fit parameters differ slightly from those of Sion et al. (1995a), due to our inclusion of the H_2 quasi-molecular satellite absorption features and a rotational broadening of 300 km s^{-1}.

boundary-layer radiation field. Since the VW Hyi boundary-layer luminosity is very low (indicating a low temperature or a nonexistent boundary layer), it is very unlikely that irradiation alone heats the belt. Instead, shear mixing or compressional heating must provide the required deep heating. Of these, shear mixing is the more efficient, i.e., provides the same degree of heating for less mass accreted than does pure radial compression. A rough estimate of the expected heating of an equatorial surface region due to axisymmetric compression by accreting matter can be made from radial accretion calculations by assuming that the amount of compressional heating scales linearly with the surface area of the accretion zone. For parameters appropriate to the superoutburst and white dwarf of VW Hyi (2 week outburst duration, 0.6 $M_\odot$ white dwarf, $\dot{M} = 1 \times 10^{-8}$ $M_\odot$ yr^{-1}, $T_{\rm eff} = 20{,}000$ K), and an assumed belt area of 10%, the model sequences of Sion (1995; Table 2) predict a belt temperature approximately 10,000 K hotter than the quiescent photosphere, or 30,000 K. This is very close to what we derive for the belt temperature from our synthetic spectral fitting of the post-SOB spectrum.

Finally, on theoretical grounds an accretion belt is plausibly expected in VW Hyi. As matter accretes tangentially at the equator, and does so every 2–3 weeks, an equilibrium state should be established such that the equatorial region spins rapidly while the higher latitudes and polar regions do not. The controlling parameter for this equilibrium state is the Richardson number, which implies a gradient of differential rotation going both inward into the white dwarf and poleward along the white dwarf surface.

We are grateful to Janet Mattei and AAVSO for their invaluable optical monitoring, required for scheduling our *Hubble Space Telescope* observation. It is a pleasure to thank Warren Sparks for useful discussions. I. H. is grateful to N. Allard for providing him with her H-quasimolecular data. This work is supported by NASA through grants GO3836.01-91A and GO6084.01-95A from the Space Telescope Science Institute, which is operated by the Association of Universities for Research in Astronomy, Inc., under NASA contract NAS5-26555. P. S. was supported by NASA LTSA grant NAGW-3158 to the University of Washington. F. H. C. is also partially supported by NASA grants GO-6019 and AR-5817.

REFERENCES

Gansicke, B., & Beuermann, K. 1996, A&A, 309, L47
Huang, M., Sion, E. M., Hubeny, I., Cheng, F. H., & Szkody, P. 1996a, ApJ, 458, 355
———. 1996b, AJ, 111, 2386
Hubeny, I. 1988, Comput. Phys. Commun. 52, 103
———. 1995, unpublished
Hubeny, I., Lanz, T., & Jeffrey, S. 1994, Newsletter on Analysis of Astronomical Spectra (St. Andrews Univ.), 20, 30
Kippenhahn, R., & Thomas, H.-C. 1978, A&A, 63, 265
Mateo, M., & Szkody, P. 1984, AJ, 89, 863
Sion, E. M. 1995, ApJ, 438, 876
Sion, E. M., Szkody, P., Cheng, F. H., & Huang, M. 1995a, ApJ, 444, L97
Sion, E. M., Huang, M., Szkody, P., & Cheng, F. H. 1995b, ApJ, 445, L31
van Amerongen, R., et al. 1987, MNRAS, 225, 93
Verbunt, F., Hassall, B., Pringle, J., Warner, B., & Marang, F. 1987, MNRAS, 225, 113